UC Irvine
UC Irvine Previously Published Works

Title

A Facile Approach for Assembling Lipid Bilayer Membranes on Template-Stripped Gold

Permalink

https://escholarship.org/uc/item/5gn4x38r

Journal

Langmuir, 26(23)

ISSN

0743-7463

Authors

Wang, Xi

Shindel, Matthew M

Wang, Szu-Wen

et al.

Publication Date

2010-12-07

DOI

10.1021/la102774n

Copyright Information

Peer reviewed

Langmuir
Article

A Facile Approach for Assembling Lipid Bilayer Membranes on Template-Stripped Gold

Xi Wang, Matthew M. Shindel, Szu-Wen Wang, and Regina Ragan*

Department of Chemical Engineering and Materials Science, University of California, Irvine, California 92697-2575, United States

Received July 11, 2010. Revised Manuscript Received October 16, 2010

Lipid vesicles are designed with functional chemical groups to promote vesicle fusion on template-stripped gold (TS Au) surfaces that does not spontaneously occur on unfunctionalized Au surfaces. Three types of vesicles were exposed to TS Au surfaces: (1) vesicles composed of only 1-palmitoyl-2-oleoyl-*sn*-glycero-3-phosphocholine (POPC) lipids; (2) vesicles composed of lipid mixtures of 2.5 mol % of 1,2-distearoyl-*sn*-glycero-3-phosphoethanolamine-*N*-poly(ethylene glycol)-2000-*N*-[3-(2-pyridyldithio)propionate] (DSPE-PEG-PDP) and 97.5 mol % of POPC; and (3) vesicles composed of 2.5 mol % of 1,2-distearoyl-*sn*-glycero-3-phosphoethanolamine-*N*-[methoxy(poly(ethylene glycol))-2000] (DSPE-PEG) and 97.5 mol % POPC. Atomic force microscopy (AFM) topography and force spectroscopy measurements acquired in a fluid environment confirmed tethered lipid bilayer membrane (tLBM) formation only for vesicles composed of 2.5 mol % DSPE-PEG-PDP/97.5 mol % POPC, thus indicating that the sulfur-containing PDP group is necessary to achieve tLBM formation on TS Au via Au-thiolate bonds. Analysis of force−distance curves for 2.5 mol % DSPE-PEG-PDP/97.5 mol % POPC tLBMs on TS Au yielded a breakthrough distance of 4.8 ± 0.4 nm, which is about 1.7 nm thicker than that of POPC lipid bilayer membrane formed on mica. Thus, the PEG group serves as a spacer layer between the tLBM and the TS Au surface. Fluorescence microscopy results indicate that these tLBMs also have greater mechanical stability than solid-supported lipid bilayer membranes made from the same vesicles on mica. The described process for assembling stable tLBMs on Au surfaces is compatible with microdispensing used in array fabrication.

Introduction

Phospholipid bilayer membranes (LBMs) have attracted considerable interest in the past few decades since their introduction as model biological membranes.[1] Planar LBMs have many applications, including biosensing platforms,[2,3] models for T-cell receptor and antigen presentation,[4,5] and platforms for studying membrane phase behavior.[6] By controlling functional membrane variables individually, LBMs provide versatile platforms for mimicking cell membranes.[7−10] Tethering LBMs using polymer supports can alleviate both immobility of transmembrane proteins and reduced lipid diffusion rates that are observed in solid supported LBMs.[7,11,12] Tethered phospholipid bilayer membranes (tLBMs) have achieved lipid diffusivity[7] comparable to that observed within cell membrane compartments measured by time-resolved diffusivity studies[13] and can yield stable membranes for electrochemical analysis.[14]

TLBMs on gold (Au) electrode surfaces, as pioneered by Spinke et al.,[15] provide a system for probing membrane−protein interactions electrochemically using impedance spectroscopy[2,16,17] and optically using techniques such as surface plasmon resonance.[2,18,19] On the basis of studies of self-assembled monolayers (SAMs) on gold, the roughness of the underlying substrate has considerable influence on molecular film defect density.[20,21] These defects are unfavorable for electrochemical analysis because they can serve as electrical short circuits. In order to overcome this problem, we use TS to produce an ultrasmooth surface[22−24] for molecular assembly since SAMs on TS Au are known to have low defect density.[25]

Vesicle fusion occurs on hydrophilic surfaces such as quartz and mica to form LBMs and has been extensively investigated and reported.[26,27] In contrast, vesicle fusion on gold surfaces typically

*Corresponding author. Telephone: (949) 824-6830; fax: (949) 824-2541; e-mail: rragan@uci.edu.

(1) Tamm, L. K.; McConnell, H. M. *Biophys. J.* **1985**, *47*(1), 105–113.
(2) Stelzle, M.; Weissmueller, G.; Sackmann, E. *J. Phys. Chem.* **1993**, *97*(12), 2974–2981.
(3) Cornell, B. A.; Braach-Maksvytis, V. L. B.; King, L. G.; Osman, P. D. J.; Raguse, B.; Wieczorek, L.; Pace, R. J. *Nature* **1997**, *387*(6633), 580–583.
(4) Brian, A. A.; McConnell, H. M. *Proc. Natl. Acad. Sci. U.S.A.* **1984**, *81*(19), 6159–6163.
(5) Grakoui, A.; Bromley, S. K.; Sumen, C.; Davis, M. M.; Shaw, A. S.; Allen, P. M.; Dustin, M. L. *Science* **1999**, *285*(5425), 221–227.
(6) Feigenson, G. W. *Biochim. Biophys. Acta* **2009**, *1788*(1), 47–52.
(7) Wagner, M. L.; Tamm, L. K. *Biophys. J.* **2000**, *79*(3), 1400–1414.
(8) Richter, R. P.; Berat, R.; Brisson, A. R. *Langmuir* **2006**, *22*(8), 3497–3505.
(9) Tanaka, M.; Sackmann, E. *Nature* **2005**, *437*(7059), 656–663.
(10) Mecke, A.; Lee, D.-K.; Ramamoorthy, A.; Orr, B. G.; Banaszak Holl, M. M. *Biophys. J.* **2005**, *89*(6), 4043–4050.
(11) Kuhner, M.; Tampe, R.; Sackmann, E. *Biophys. J.* **1994**, *67*(1), 217–226.
(12) Naumann, C. A.; Prucker, O.; Lehmann, T.; Ruhe, J.; Knoll, W.; Frank, C. W. *Biomacromolecules* **2001**, *3*(1), 27–35.
(13) Fujiwara, T.; Ritchie, K.; Murakoshi, H.; Jacobson, K.; Kusumi, A. *J. Cell Biol.* **2002**, *157*(6), 1071–1082.
(14) Lin, J.; Szymanski, J.; Searson, P. C.; Hristova, K. *Langmuir* **2010**, *26*(5), 3544–3548.
(15) Spinke, J.; Yang, J.; Wolf, H.; Liley, M.; Ringsdorf, H.; Knoll, W. *Biophys. J.* **1992**, *63*(6), 1667–1671.
(16) Raguse, B.; Braach-Maksvytis, V.; Cornell, B. A.; King, L. G.; Osman, P. D. J.; Pace, R. J.; Wieczorek, L. *Langmuir* **1998**, *14*(3), 648–659.
(17) Yin, P.; Burns, C. J.; Osman, P. D. J.; Cornell, B. A. *Biosens. Bioelectron.* **2003**, *18*(4), 389–397.
(18) Knoll, W.; Koper, I.; Naumann, R.; Sinner, E.-K. *Electrochim. Acta* **2008**, *53*(23), 6680–6689.
(19) Munro, J. C.; Frank, C. W. *Langmuir* **2004**, *20*(24), 10567–10575.
(20) Losic, D.; Shapter, J. G.; Gooding, J. J. *Langmuir* **2001**, *17*(11), 3307–3316.
(21) Leopold, M. C.; Black, J. A.; Bowden, E. F. *Langmuir* **2002**, *18*(4), 978–980.
(22) Schiller, S. M.; Naumann, R.; Lovejoy, K.; Kunz, H.; Knoll, W. *Angew. Chem., Int. Ed.* **2003**, *42*(2), 208–211.
(23) Duati, M.; Grave, C.; Tcbeborateva, N.; Wu, J.; Mullen, K.; Shaporenko, A.; Zharnikov, M.; Kriebel, J. K.; Whitesides, G. M.; Rampi, M. A. *Adv. Mater.* **2006**, *18*(3), 329–333.
(24) Ragan, R.; Ohlberg, D.; Blackstock, J. J.; Kim, S.; Williams, R. S. *J. Phys. Chem. B* **2004**, *108*(52), 20187–20192.
(25) Lee, L.; Bae, S.-S.; Medeiros-Ribeiro, G.; Blackstock, J. J.; Kim, S.; Stewart, D. R.; Ragan, R. *Langmuir* **2008**, *24*(12), 5984–5987.
(26) Kalb, E.; Frey, S.; Tamm, L. K. *Biochim. Biophys. Acta* **1992**, *1103*(2), 307–316.

requires chemical functionalization of the gold surface.[28,29] Fabrication of tLBMs on gold thus requires multiple preparation steps, mainly using a combination of Langmuir−Blodgett transfer and vesicle fusion[7,30] or a combination of Langmuir−Blodgett and Langmuir−Schaefer transfer,[12] or requiring gold surface modification[2,30,31] prior to vesicle fusion. For example, Giess et al. utilized proteins as tethering groups in tLBMs, which require a gold chelating surface.[32] Here, we demonstrate that tLBMs are able to form on unfunctionalized TS Au surfaces using phospholipid vesicles composed of 1-palmitoyl-2-oleoyl-*sn*-glycero-3-phosphocholine (POPC) and 1,2-distearoyl-*sn*-glycero-3-phosphoethanolamine-*N*-poly(ethylene glycol)-2000-*N*-[3-(2-pyridyldithio)propionate] (DSPE-PEG-PDP) mixtures. Samples were characterized using atomic force microscopy (AFM) and fluorescence microscopy under aqueous conditions. AFM has been extensively used to investigate LBM topography[8,33−35] due to its ability to acquire nanometer-resolution images under physiological conditions.[36,37] AFM topography images and force spectroscopy measurements confirm the presence of tLBMs on TS Au for vesicles composed of 2.5% DSPE-PEG-PDP/97.5% POPC. DSPE-PEG-PDP was incorporated to form a Au-thiolate bond[31] with gold surfaces in order to facilitate vesicle fusion on TS Au. Furthermore, stability of tLBMs was found to be relatively higher than that of solid supported LBMs on mica. Thus, the fabrication process introduced in this work yields stable tLBMs on TS Au without an additional processing step to functionalize TS Au substrates.

Experimental Section

Materials. 1-Palmitoyl-2-oleoyl-*sn*-glycero-3-phosphocholine (POPC), 1,2-distearoyl-*sn*-glycero-3-phosphoethanolamine-*N*-poly(ethylene glycol)-2000-*N*-[3-(2-pyridyldithio)propionate] (DSPE-PEG-PDP), 1,2-distearoyl-*sn*-glycero-3-phosphoethanolamine-*N*-[methoxy(poly(ethylene glycol))-2000] (DSPE-PEG), and fluorescence probe 1,2-dipalmitoyl-*sn*-glycero-3-phosphoethanolamine-*N*-(7-nitro-2-1,3-benzoxadiazol-4-yl) (NBD-DPPE) were purchased from Avanti Polar Lipids (Alabaster, AL). Molecular structures of POPC, DSPE-PEG-PDP, DSPE-PEG, and NBD-DPPE are shown in Figure 1. NaCl at >99.0% purity was obtained from Fisher Scientific Inc. (Pittsburgh, PA). HEPES at >99.5% purity and chloroform at >99.8% purity were purchased from Sigma-Aldrich (St. Louis, MO). V-1 quality mica was supplied by Ted Pella Inc. (Redding, CA). All water used in this study was obtained using a Milli-Q water system (≥ 18.2 MΩ. cm, Millipore Corp., Billerica, MA). Silicon wafers were purchased from University Wafer (South Boston, MA). EPO-TEK 377H, two-component epoxy glue, was purchased from Epoxy Technology, Inc., (Billerica, MA) and was used for fabricating TS Au surfaces.

Preparation of Template-Stripped Gold (TS Au) Surfaces. TS Au surfaces were prepared using a simplified protocol from that reported by Lee et al.[25] Gold films (1000 nm thick) were
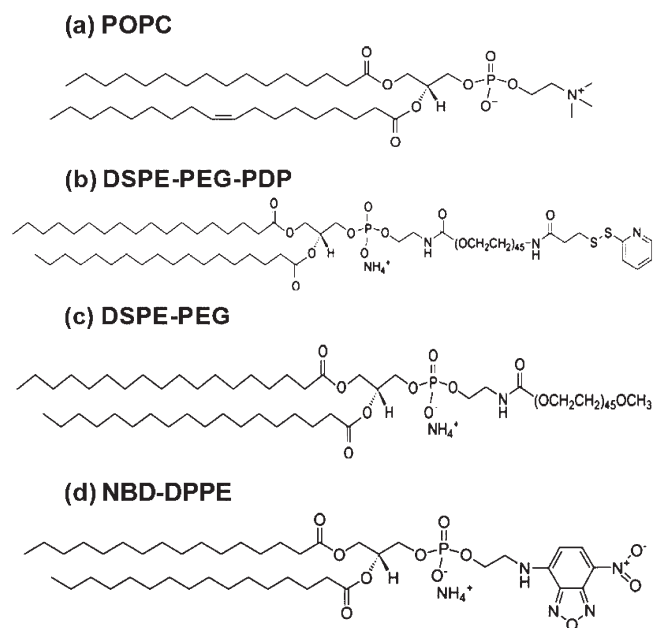
Figure 1. Chemical structure of lipids used in this study: (a) POPC is the primary component in tLBMs; (b) DSPE-PEG-PDP molecule with disulfide group is used for Au-thiolate bond formation; (c) DSPE-PEG without the disulfide group is used as a control molecule; (d) NBD-DPPE is used as a fluorescence probe.

deposited by electron beam deposition (rate 1−3 nm/s, 2×10^{-6} Torr) on silicon templates which had a thermally oxidized SiO$_x$ layer approximately 2.7 nm thick. Prior to stripping, gold on silicon templates was annealed at 200 °C for 24 h under ambient conditions to facilitate grain growth and decrease surface roughness.[24,25] Gold surfaces were then glued with EPO-TEK 377H to silicon substrates, forming a sandwich structure, and cured at 200 °C for 1 h. After cooling, silicon templates were detached from silicon substrates to expose a TS Au film with a root-mean-square roughness less than 0.6 nm over $2 \mu m \times 2 \mu m$ as evaluated by AFM. TS Au films used as substrates for tLBMs were used immediately after stripping to maintain a pristine surface for membrane assembly.

Preparation of Unilamellar Vesicles. Large unilamellar vesicles were prepared by a standard extrusion method.[7,26] Stock solutions of lipids at concentrations of 1 mg/mL in chloroform were dried on the bottom of a glass vial by a gentle stream of nitrogen and desiccated under vacuum for at least 1 h. The dried lipid mixtures were then rehydrated by the addition of HEPES buffer (5 mM HEPES, pH 7.4, containing 150 mM NaCl) to yield a final lipid concentration of 5 mM. The resulting lipid suspensions were then vortexed, subjected to five freeze−thaw cycles, and extruded eleven times through two polycarbonate membranes of 100 nm pore size using a syringe-type extruder (Avanti Polar Lipids, Alabaster, AL). The size of vesicles was measured by dynamic light scattering (Malvern Zetasizer ZS) to have an average diameter of 120 nm with a polydispersity index less than 0.2.

Preparation of Lipid Bilayer Membranes (LBMs). Three types of substrates were used in this study: freshly cleaved mica, freshly stripped TS Au, and oxygen plasma cleaned TS Au. Oxygen plasma cleaning of TS Au was performed for 5 min at a vapor pressure of 200 mTorr using a PC2000 plasma cleaner (South Bay Technology Inc., San Clemente, CA). This produced a hydrophilic surface with a contact wetting angle of less than 10°. Vesicles composed of 2.5% DSPE-PEG-PDP/97.5% POPC lipids were deposited on TS Au and mica. Control samples included vesicles composed of 100% POPC deposited on mica, TS Au, and oxygen plasma cleaned TS Au and vesicles composed of 2.5% DSPE-PEG/97.5% POPC deposited on TS Au.

(27) Reviakine, I.; Bergsma-Schutter, W.; Brisson, A. *J. Struct. Biol.* **1998**, *121*(3), 356−361.
(28) Ekeroth, J.; Konradsson, P.; Hook, F. *Langmuir* **2002**, *18*(21), 7923−7929.
(29) Wiegand, G.; Arribas-Layton, N.; Hillebrandt, H.; Sackmann, E.; Wagner, P. *J. Phys. Chem. B* **2002**, *106*(16), 4245−4254.
(30) Shen, W. W.; Boxer, S. G.; Knoll, W.; Frank, C. W. *Biomacromolecules* **2000**, *2*(1), 70−79.
(31) Munro, J. C.; Frank, C. W. *Langmuir* **2004**, *20*(8), 3339−3349.
(32) Giess, F.; Friedrich, M. G.; Heberle, J.; Naumann, R. L.; Knoll, W. *Biophys. J.* **2004**, *87*(5), 3213−3220.
(33) Chen, M.; Li, M.; Brosseau, C. L.; Lipkowski, J. *Langmuir* **2009**, *25*(2), 1028−1037.
(34) Li, M.; Chen, M.; Sheepwash, E.; Brosseau, C. L.; Li, H.; Pettinger, B.; Gruler, H.; Lipkowski, J. *Langmuir* **2008**, *24*(18), 10313−10323.
(35) Jass, J.; Tjarnhage, T.; Puu, G. *Biophys. J.* **2000**, *79*(6), 3153−3163.
(36) Kada, G.; Kienberger, F.; Hinterdorfer, P. *Nano Today* **2008**, *3*(1−2), 12−19.
(37) Dufrene, Y. F.; Lee, G. U. *Biochim. Biophys. Acta* **2000**, *1509*(1−2), 14−41.
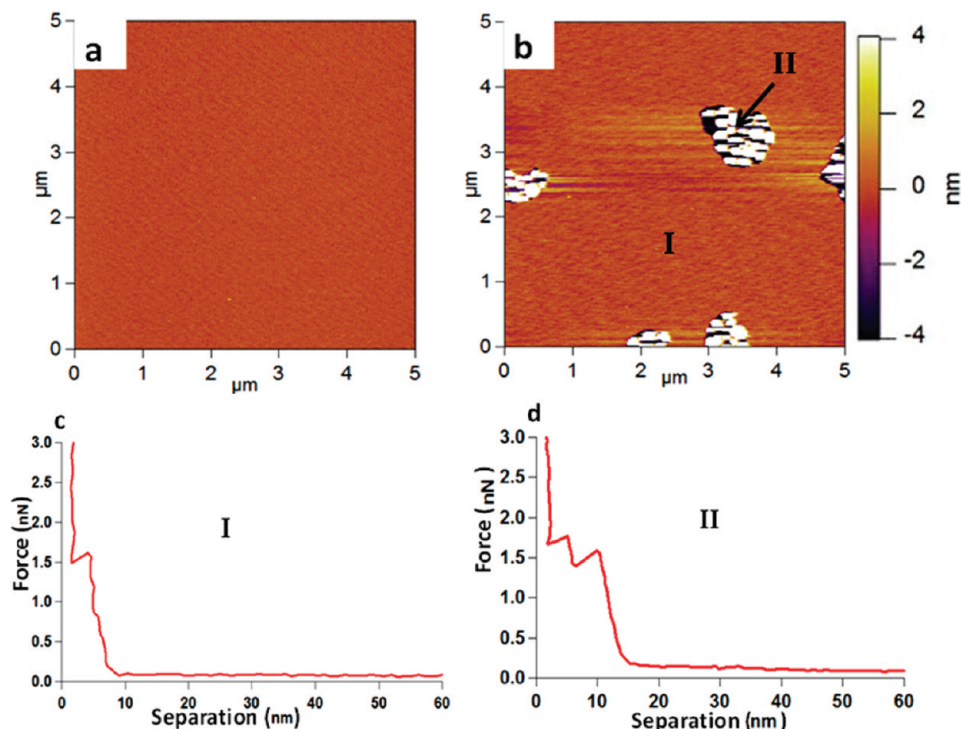
Figure 2. AFM topography images of mica (a) before and (b) after incubation with pure POPC vesicles in solution. Representative force−distance curves that were obtained from (c) region I and (d) region II, as labeled in panel (b).

All samples were prepared using the following procedure. A 150 μL suspension of vesicles in HEPES buffer was deposited on 8 mm × 8 mm substrates that were glued onto glass slides. After a 30 min incubation period, surfaces were rinsed with 200 μL of HEPES buffer twice. HEPES buffer (150 μL) was added to the surfaces to keep them hydrated, and the samples were further characterized.

Atomic Force Microscopy (AFM). Both AFM topography images and force−distance curves were obtained using a MFP-3D-Bio atomic force microscope (Asylum Research, Santa Barbara, CA). Commercial pyramid-shaped Si_3N_4 cantilever tips (OMCL-TR400PSA, Olympus) with a nominal spring constant of 0.08 N/m were used. AFM images were acquired at room temperature in HEPES buffer using tapping mode at a scan speed of 1.0 Hz. All images contain 512 × 512 pixels and were rendered using *Igor Pro* software v 6.0 with background slopes corrected. Force spectroscopy was performed under contact mode in HEPES buffer. In force spectroscopy, as the AFM tip approaches a plastically deformable membrane on a hard surface, a discontinuity occurs in the approaching force−distance curve as the tip penetrates the membrane surface. The horizontal distance measured from the onset of the discontinuity to the hard surface repulsive curve is referred to as the breakthrough distance and is related to the membrane thickness.[34,38,39] Multiple force−distance curves were obtained for each sample to ensure representative data.

Fluorescence Microscopy. In order to examine membrane stability, LBMs composed of 2.5% DSPE-PEG-PDP, 2% NBD-DPPE, and 95.5% POPC were prepared on TS Au (tethered) and on mica (untethered control), as described above. Fluorescence micrographs were taken with an Olympus BX51 fluorescence microscopy with a cooled CCD camera (ORCA-285, Hamamatsu), and all samples were immersed in water during imaging. Images were obtained before and after multiple rigorous washings with Milli-Q water. In order to compare fluorescence intensity values among different images, the autointensity function of the digital

camera was turned off and pixel intensities within each image were averaged.

Results and Discussion

Deposition of POPC Vesicles on Mica and TS Au. Mica has been used extensively as a substrate for LBM formation due to its ultraflat, hydrophilic surface,[8,38,40−42] and POPC vesicle fusion on mica has been extensively investigated. Therefore, we examined solid-supported LBMs (without tethering groups) on mica in order to compare with tLBMs on TS Au surfaces. Figure 2a,b are 5 μm × 5 μm AFM topography images of mica before and after exposure to vesicles comprising pure POPC, respectively. After vesicle exposure, the surface shown in Figure 2b exhibits flat featureless regions (labeled "I") and a few bright regions (labeled "II").

Force spectroscopy was performed on regions I and II as labeled in Figure 2b, and representative force−distance curves exhibiting single breakthrough events (region I) and multiple breakthrough events (region II) are shown in Figure 2c and d, respectively. Note that force−distance curves were also obtained on bare mica substrates and show no breakthrough events (Supporting Information, Figure S1). Data from force−distance curves acquired on region I provided an average breakthrough distance for single breakthrough events to be 3.1 ± 0.6 nm ($n = 146$ curves); the breakthrough distance agrees with previously measured values for a POPC bilayer on mica.[43] The standard deviation of the breakthrough distance is influenced by the fluid nature of the membrane and the statistical nature of the breakthrough event.[40,44]

(38) Garcia-Manyes, S.; Oncins, G.; Sanz, F. *Biophys. J.* **2005**, *89*(3), 1812–1826.
(39) Garcia-Manyes, S.; Oncins, G.; Sanz, F. *Electrochim. Acta* **2006**, *51*(24), 5029–5036.

(40) Franz, V.; Loi, S.; Muller, H.; Bamberg, E.; Butt, H.-J. *Colloids Surf., B* **2002**, *23*(2−3), 191–200.
(41) Oncins, G.; Garcia-Manyes, S.; Sanz, F. *Langmuir* **2005**, *21*(16), 7373–7379.
(42) Dufrene, Y. F.; Barger, W. R.; Green, J.-B. D.; Lee, G. U. *Langmuir* **1997**, *13*(18), 4779–4784.
(43) Canale, C.; Jacono, M.; Diaspro, A.; Dante, S. *Microsc. Res. Technol.* **2010**, *73*(10), 965–972.
(44) Choi, E. J.; Dimitriadis, E. K. *Biophys. J.* **2004**, *87*(5), 3234–3241.
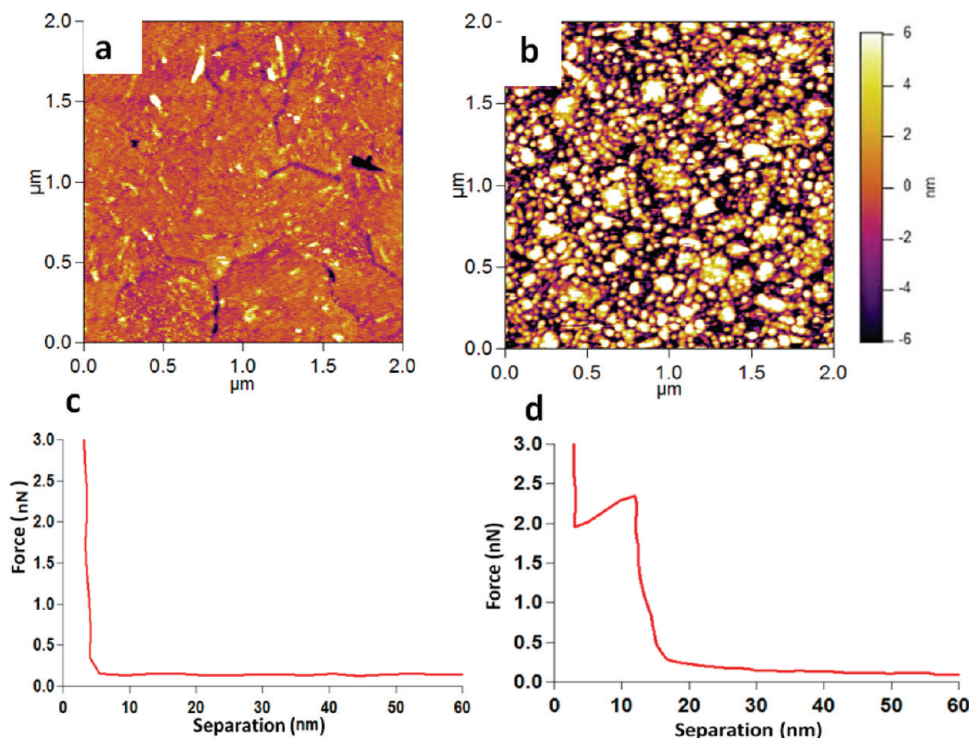
Figure 3. AFM topography images after deposition of pure POPC vesicles on (a) TS Au and (b) plasma cleaned TS Au. (c,d) Typical force–distance curves acquired in the scanning regions of (a) and (b), respectively.

The expected membrane thickness of a LBM composed of lipids with 16–18 carbon–carbon bonds in the hydrophobic chains is approximately 3.7 nm.[45] The breakthrough distance is related to the thickness of a compressed LBM due to elastic deformation of a LBM induced by an AFM probe prior to breakthrough and thus is expected to be slightly smaller than the thickness of a LBM at equilibrium.[33,46,47] Therefore, force spectroscopy measurements indicate there is a single LBM on region I.

The yield threshold force at which breakthrough occurs in the force–distance curves from region I was also measured, and the average value was calculated to be 1.4 ± 0.2 nN ($n = 146$ curves). Double breakthrough (triple-breakthrough) events were typically (infrequently) observed on force–distance curves obtained in region II (Figure 2d) that are consistent with multilayer formation on mica. The breakthrough distances for a double breakthrough event in the force–distance curve shown in Figure 2d are 3.3 and 3.4 nm, indicating the presence of two LBMs, and the corresponding yield threshold forces for these events are 1.7 nN and 1.5 nN, respectively. The majority of the mica surface is covered by regions of type I (single LBM) and a few regions of type II (multiple LBMs).

POPC vesicles were then deposited on TS Au. An AFM topography image of the surface after exposure to POPC vesicles is shown in Figure 3a, with a corresponding representative force–distance curve shown in Figure 3c. The force–distance curve indicates a tip interaction with a hard surface and shows no breakthrough; thus, there is no evidence that a LBM is formed on TS Au. The absence of LBM formation on TS Au is consistent with previous studies where vesicle fusion does not take place on unfunctionalized Au surfaces.[48] Since the hydrophilicity of mica

surfaces is a factor for vesicle fusion,[8,49] TS Au substrates were treated with oxygen plasma to produce a hydrophilic TS Au surface. After plasma cleaning, the contact wetting angle of TS Au decreased from approximately 75° to less than 10°, indicating hydrophilicity. Figure 3b shows an AFM topography image of plasma-cleaned TS Au after exposure to a solution of vesicles comprising 100% POPC. The rounded features in Figure 3b appear to be adsorbed vesicles on the surface, since they are much thicker than a POPC LBM. A representative force–distance curve measured on this sample is shown in Figure 3d and exhibits a breakthrough distance of 8.9 nm that is also in agreement with adsorbed vesicles on the surface. No evidence of vesicle rupture and LBM formation was observed in AFM images and force spectroscopy measurements. This result is consistent with previous studies that show intact vesicles adsorb on hydrophilic gold surfaces without LBM formation, and simply the presence of a hydrophilic surface is not sufficient for vesicle fusion.[48,50]

Deposition of 2.5% DSPE-PEG-PDP/97.5% POPC Vesicles on Mica and TS Au. Vesicles composed of 2.5% DSPE-PEG-PDP/97.5% POPC were deposited on TS Au. As shown in Figure 1b, DSPE-PEG-PDP has a disulfide group that is incorporated for Au-thiolate bond formation at the surface.[19,31,51] Figure 4a,b show 5 μm × 5 μm AFM topography images of TS Au before and after exposure to 2.5% DSPE-PEG-PDP/97.5% POPC vesicles, respectively. The topography image of Figure 4b has a similar appearance as the bare TS Au surface (shown in Figure 4a) but slightly higher root-mean-square roughness. Vesicles composed of 2.5% DSPE-PEG-PDP/97.5% POPC were also deposited on mica for comparison and AFM topography images confirmed LBM formation. (Supporting Information, Figure S2).

Force–distance curves were acquired on the area shown in Figure 4b (after exposure to 2.5% DSPE-PEG-PDP/97.5% POPC vesicles) and exhibited single breakthrough events and a

(45) Lewis, B. A.; Engelman, D. M. *J. Mol. Biol.* **1983**, *166*(2), 211–217.
(46) Butt, H.-J.; Stark, R. *Colloid. Surf., A* **2005**, *252*(2–3), 165–168.
(47) Garcia-Manyes, S.; Sanz, F. *Biochim. Biophys. Acta* **2010**, *1798*(4), 741–749.
(48) Reimhult, E.; Hook, F.; Kasemo, B. *Langmuir* **2003**, *19*(5), 1681–1691.
(49) Zhdanov, V. P.; Kasemo, B. *Langmuir* **2001**, *17*(12), 3518–3521.

(50) Keller, C. A.; Kasemo, B. *Biophys. J.* **1998**, *75*(3), 1397–1402.
(51) Biebuyck, H. A.; Whitesides, G. M. *Langmuir* **1993**, *9*(7), 1766–1770.
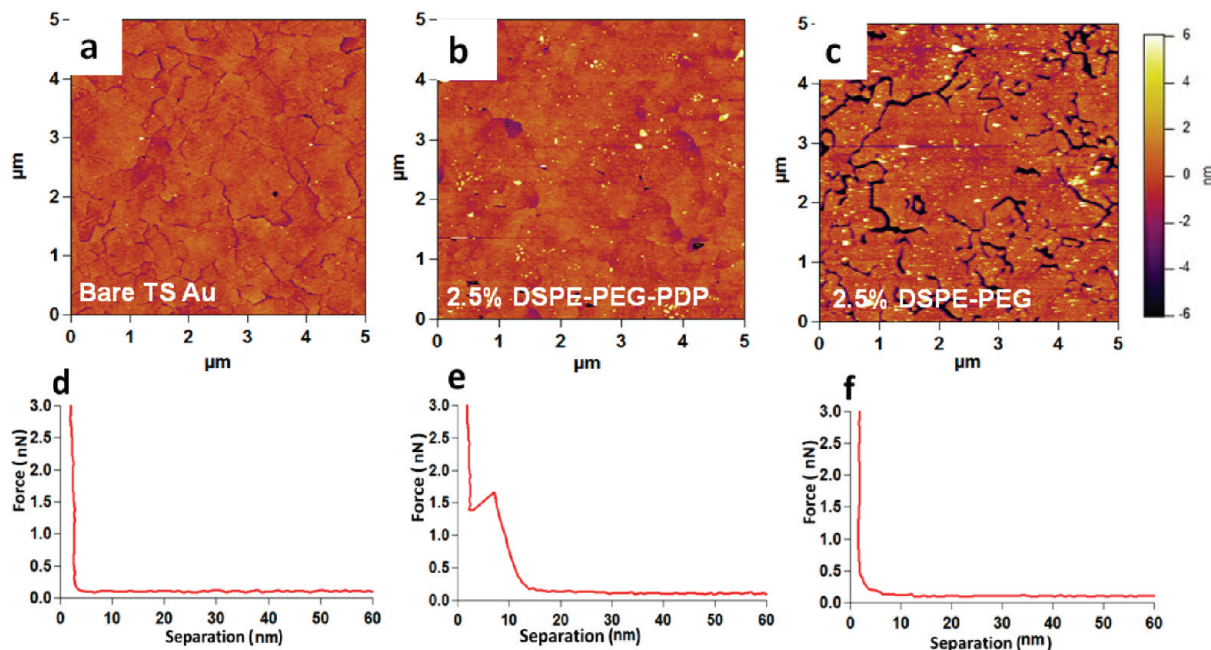
Figure 4. AFM topography images of (a) bare TS Au, (b) TS Au after incubation with vesicles composed of 2.5% DSPE-PEG-PDP/97.5% POPC, and (c) TS Au after incubation with vesicles composed of 2.5% DSPE-PEG/97.5% POPC. Panels (d), (e), and (f) are typical force−distance curves obtained from the scanning regions shown in (a), (b), and (c), respectively.

typical force curve shown in Figure 4e. Analysis of these collected force−distance curves after vesicle incubation on TS Au provided an average breakthrough distance of 4.8 ± 0.4 nm (n = 158 curves) and a yield threshold force of 1.3 ± 0.2 nN (n = 158 curves). This calculated average breakthrough distance of the tLBM (4.8 ± 0.4 nm) is approximately 1.7 nm larger than that of the solid-supported POPC LBM on mica (3.1 ± 0.6 nm). In comparison force spectroscopy, on the bare TS Au control showed no breakthrough events (Figure 4d) as expected. AFM topography was also used to measure tLBM thickness and the average height is consistent with the breakthrough distance of tLBMs measured by force spectroscopy (Supporting Information, Figure S3).

The larger breakthrough distance for 2.5% DSPE-PEG-PDP/ 97.5% POPC on TS Au relative to POPC on mica is attributed to the presence of the PEG group. The tLBM resulting from the assembly process is expected to be composed of essentially two identical lipid monolayers inverted relative to each other. The PEG groups from the molecules in the inner leaflet (those facing the substrate) are expected to be covalently bound to the TS Au by thiolate chemistry. These PEG chains are also expected to provide some additional space (a cushion) between the membrane and the TS Au support. This is consistent with the tLBM structure proposed in previous work[7,52] where a PEG tether was functionalized for covalent attachment to silicate surfaces.

In order to evaluate the importance of the PDP group on tLBM formation, vesicles composed of 2.5% DSPE-PEG/97.5% POPC were also deposited on TS Au and characterized with AFM. A 5 μm × 5 μm AFM image of vesicles composed of 2.5% DSPE-PEG/97.5% POPC deposited on TS Au is shown in Figure 4c; no evidence of intact vesicle adsorption or vesicle fusion is observed. Since DSPE-PEG does not have a functional group to form a thiolate bond with TS Au, a strong interaction between DSPE-PEG and TS Au is not expected. Force−distance curves (Figure 4f) are similar to that of the bare TS Au surface

(Figure 4d); there is no evidence of LBM formation. Thus, by comparison of these results with the AFM results for 2.5% DSPE-PEG-PDP/97.5% POPC, it is evident that functional PDP groups are important for tLBM formation on TS Au. Overall, the results indicate that Au-thiolate bonds between DSPE-PEG-PDP and TS Au are critical for promoting vesicle rupture and fusion on TS Au surfaces.

Fluorescence Microscopy. Fluorescence microscopy was also utilized to characterize tLBM formation on TS Au and specifically to compare tLBM stability on TS Au and LBM stability on mica. Vesicles composed of 2.5% DSPE-PEG-PDP, 2% NBD-DPPE fluorescence label, and 95.5% POPC were deposited on TS Au. A uniform fluorescence signal was observed, which is an indicator of homogeneous tLBM coverage on TS Au (Supporting Information, Figure S4a). In order to provide a reference point, a hole was scratched into the tLBM. The dark regions associated with the reference point are highlighted by red arrows in Figure 5a−c. When the tLBM was rinsed once and then twice with water, the fluorescence intensity of the tLBM was still uniform as shown in Figure 5b,c, respectively. The measured fluorescence intensity thus demonstrates that the tLBM was still present on the TS Au after rinsing. After additional multiple washings, fluorescence intensity was still observable on the tLBM on TS Au (Supporting Information, Figure S4b). In comparison, uniform fluorescence was also observed on the LBM prepared by fusion of vesicles composed of 2.5% DSPE-PEG-PDP, 2% NBD-DPPE fluorescence label, and 95.5% POPC on mica before rinsing (Figure 5d). Yet after rinsing with water only once, the fluorescence intensity of the LBM on mica became inhomogeneous (Figure 5e). Thus, regions of the LBM appear to have been removed due to rinsing. After rinsing twice, there was a further significant decrease in fluorescence intensity, indicating further removal of LBM regions on mica (Figure 5f).

The relative, mean fluorescence intensity across the entire image as a function of rinsing for both mica and TS Au surfaces was compared by plotting the mean gray-scale intensity values corresponding to the fluorescence images in Figure 5a−f. This

(52) Naumann, C. A.; Prucker, O.; Lehmann, T.; Ruhe, J.; Knoll, W.; Frank, C. W. *Biomacromolecules* **2002**, *3*(1), 27–35.
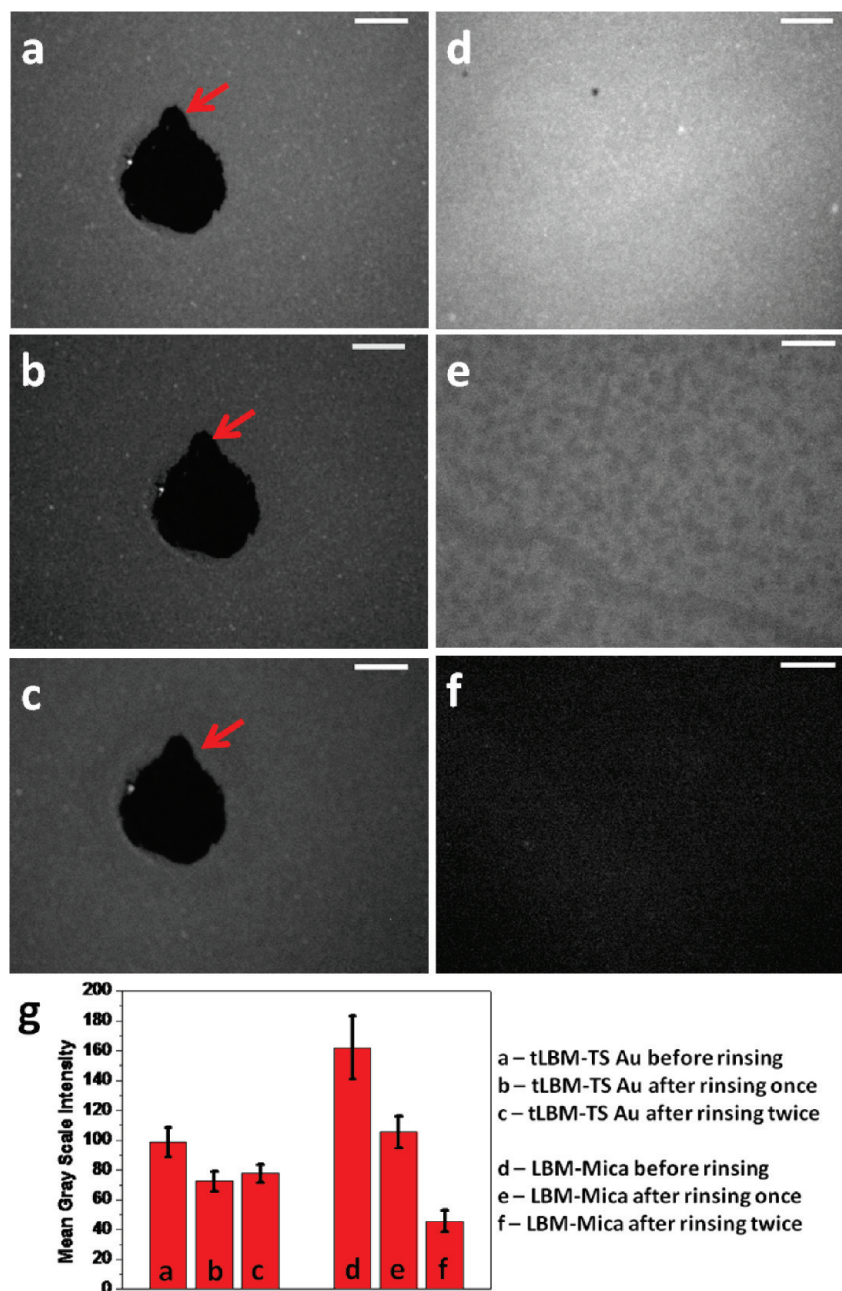
Figure 5. Fluorescence images are shown of 2.5% DSPE-PEG-PDP, 2% NBD-DPPE, and 95.5% POPC tLBM on TS Au (a) before rinsing, (b) after rinsing with water once, and (c) after rinsing with water twice. (The red arrows mark a position scratched by a pair of tweezers that is used as a reference point.) As a control, fluorescence images are shown of (d) 2.5% DSPE-PEG-PDP, 2% NBD-DPPE, and 95.5% POPC LBM on mica (d) before rinsing, (e) after rinsing with water once, and (f) after rinsing with water twice. The scale bar in all fluorescence images is 100 μm. (g) A bar chart of mean gray-scale intensity values corresponding to fluorescence images in (a) to (f). The error bar represents the standard deviation of mean gray-scale intensity values of the pixels in each fluorescence images (excluding the reference points highlighted with the arrows).

data is presented in the bar chart of Figure 5g. Generally, fluorescence intensity before rinsing of the LBM on mica is higher than that of the tLBM on TS Au, likely due to partial quenching of the fluorescence intensity signal due to the TS Au surface.[53] It is significant that the fluorescence intensity of the LBM on mica became inhomogeneous after the first rinsing step when compared to the intensity before rinsing; this is observable in both the image of Figure 5e and the decrease in mean intensity value. Topography changes due to successive rinses were also evaluated by AFM

(Supporting Information, Figure S5). The AFM images support the fluorescence data and show that the LBM is partially removed after each rinsing step. Before rinsing, force−distance curves obtained in the region showed consistent breakthrough events, and a representative force−distance curve is shown in Supporting Information Figure S5a(I). After rinsing with water once (Supporting Information Figure S5b(I)), AFM topography shows inhomogeneous surface coverage with two typical features marked with (II) and (III). Force−distance curves obtained on feature (II) showed consistent breakthrough events, indicating that these domains are LBM patches. In contrast, force−distance curves obtained on feature (III) did not show breakthrough

(53) Lee, C.-Y.; Gong, P.; Harbers, G. M.; Grainger, D. W.; Castner, D. G.; Gamble, L. J. *Anal. Chem.* **2006**, *78*(10), 3316–3325.

events, indicating that these regions are exposed to bare mica due to partial removal of the LBM from mica as a result of rinsing. After rinsing with water twice, AFM topography image (Supporting Information Figure S5c(I)) shows only a few features that appear to be LBMs having lateral width less than 100 nm. Typical force−distance curve shown in Supporting Information Figure S5(IV) do not exhibit breakthrough events, implying that the majority of the LBM delaminated after two rinsing steps.

Since the PDP group does not react with mica, the DSPE-PEG-PDP group does not act as a tether to the surface and cannot help to stabilize the LBM during rinsing. In contrast, the fluorescence intensity of the tLBM on TS Au underwent a smaller decrease after rinsing; the difference before and after rinsing is slightly lower than the standard deviation of the mean gray-scale values in the image. The slight decrease in intensity after the first rinsing step is likely due to removal of some of the fluorescent tagged lipids that are nonspecifically bound on the surface; there is no decrease in fluorescence intensity after the second rinsing step, suggesting that there is no further removal of adsorbed lipids. Thus, these results indicate that the interaction between the disulfide group of PEG-PDP and the TS Au surface appears to stabilize the tLBM on TS Au.

Conclusion

Our work here demonstrates that tLBMs can be assembled on unfunctionalized TS Au surfaces by incorporating a disulfide functionalized lipid group in low quantities in vesicles prior to vesicle fusion. AFM topography images and force spectroscopy demonstrated that tLBMs formed over 25 μm^2 areas on TS Au. The yield threshold force needed for an AFM tip to penetrate tLBMs (1.3 ± 0.2 nN) is similar with that measured on POPC LBMs on mica (1.4 ± 0.2 nN), while the breakthrough distances of tLBMs determined from force−distance curves is about 1.7 nm thicker than solid-supported LBMs due to the presence of DSPE-PEG-PDP in the tLBMs. Fluorescence analysis further demonstrated that tLBMs on TS Au are a robust membrane system that is stable to solution exchange such as used in protein analysis. The template-stripping process produces ultraflat TS Au surfaces that are favorable for low defect density membrane formation. Our process shows promise to obtain biomimetic membranes on Au surfaces. However, further refinement of the deposition methods is needed to minimize defect density. Future work includes optimization of TS Au surface preparation and membrane incubation parameters. Furthermore, pipet dispensing of vesicles to form robust tLBMs on TS Au is an approach with potential to integrate with noncontact microarray technology.

Supporting Information Available: S1: Representative force−distance curve obtained on bare mica. S2: AFM topography image and corresponding height-distance profile of a mica surface after exposure to vesicles composed of 2.5% DSPE-PEG-PDP/97.5% POPC. S3: AFM topography image and corresponding height−distance profile of tLBM with sub-monolayer coverage on TS Au prepared by vesicles composed of 2.5% DSPE-PEG-PDP/97.5% POPC (0.5 μmol/mL). S4: Fluorescence images of 2.5% DSPE-PEG-PDP/97.5% POPC tLBM on TS Au before rinsing and after multiple rinsing steps. S5: AFM topography images recording of mica after exposure to vesicles composed of 2.5% DSPE-PEG-PDP/97.5% POPC experiencing rinsing steps (before rinsing, after rinsing once and after rinsing twice). This material is available free of charge via the Internet at http://pubs.acs.org.